IAWA Journal 37 (1), 2016: 28–47

BRILL

COMPUTED TOMOGRAPHY AND LIGHT MICROSCOPY: COMBINING VISUALISATION TECHNIQUES IN THE STUDY OF MANGROVE SEEDLING DEVELOPMENT

Nathalie Tonné[1,2,*], **Nico Koedam**[1], **Nico Buls**[3], **Johan De Mey**[3], **Hans Beeckman**[2] and **Elisabeth M.R. Robert**[1,2]

[1]Laboratory of Plant Biology and Nature Management (APNA), Vrije Universiteit Brussel, Pleinlaan 2, B-1050 Brussels, Belgium
[2]Laboratory of Wood Biology and Xylarium, Royal Museum for Central Africa (RMCA), Leuvensesteenweg 13, B-3080 Tervuren, Belgium
[3]Radiology, Universitair Ziekenhuis Brussel (UZ Brussel), and BEFY-LABO, Vrije Universiteit Brussel, Laarbeeklaan 101, B-1090 Brussels, Belgium
*Corresponding author: e-mail: ntonne@vub.ac.be

ABSTRACT

When seedlings grow into young plants their tissue proportions change over time. Viviparous mangrove seedlings of the Rhizophoraceae are different from other young trees. They consist of a thickened cylinder-shaped hypocotyl that allows the seedlings to float and disperse before establishment. Despite the crucial role in the ecological and biogeographical success of mangroves, not much has been published about the internal development of mangrove seedlings in their early life stages. We used X-ray CT-scanning and light microscopy to investigate the internal development (i) over time and (ii) with hypocotyl height in seedlings of the mangrove species *Bruguiera gymnorrhiza* and *Ceriops tagal*. While light microscopy offered cell- and tissue identification in destructive transverse sections, X-ray CT-scanning allowed investigating the internal tissue development of living plants over time in a non-destructive way. Our results indicated that the vascular tissue proportionally increased over time and with hypocotyl height in both species in accordance with the growing importance of this tissue in the developing seedlings. As a result, the cortex, composed of an inner and outer zone, proportionally decreased over time and with height in both species. No clear trends over time and with height could be observed regarding the proportion of the pith tissue. A decrease in average density of all tissues together with height was discerned in both species indicating the seedlings were heavier at their base. The latter suggests a supporting role of the seedling base in tidal and wind action. The combination of CT-scanning and light microscopy offered the advantages of both methods in the developmental study of young mangrove plants, and opens perspectives in the study of internal development of young plants in general.

Keywords: *Bruguiera gymnorrhiza*, *Ceriops tagal*, destructive and non-destructive seedling anatomy analysis with time and height, hypocotyl tissue proportions.

DOI 10.1163/22941932-20160119

INTRODUCTION

During the development of most eudicot seedlings to young trees, plants build a ring of vascular tissue consisting of vascular bundles. The vascular bundles unite forming a vascular cylinder that subsequently increases during radial (secondary) growth initiated at the vascular cambium (Ye 2002; Evert 2006). During secondary growth, the

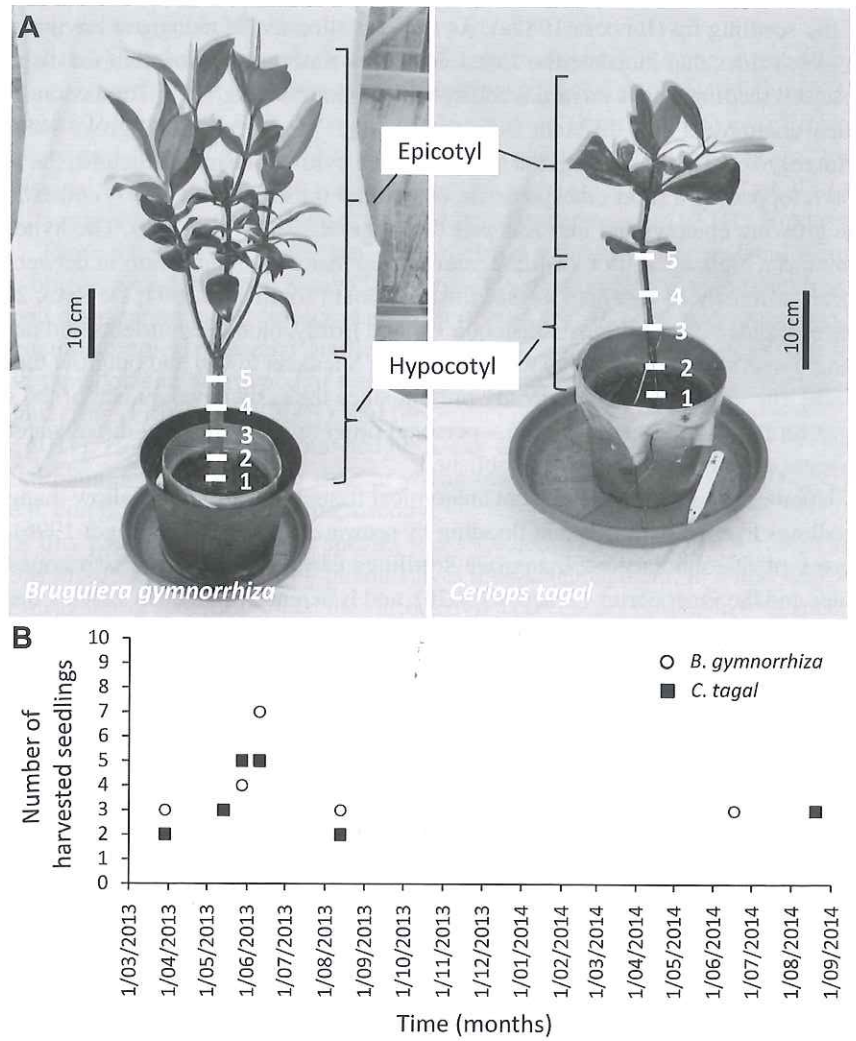

Figure 1. – A: Pictures of the CT-analysed *Bruguiera gymnorrhiza* (left) and *Ceriops tagal* (right) seedlings on which the hypocotyl and epicotyl parts of the plants and the analysed heights in the aboveground hypocotyl part of the seedlings are indicated. Both plants were collected and potted in January 2013. Photographs were taken on 14 August 2014. – B: Number of seedlings of each species harvested in 2013 and 2014. Plants were potted in January and February 2013, except for one *B. gymnorrhiza* seedling that was potted in April 2013.

secondary xylem completely surrounds the primary xylem and pith, while the tissues outside the vascular cambium are forced outward (Evert 2006). As a result the tissue proportions within the stem of young woody plants change over time.

Young plants of viviparous mangrove species belonging to the Rhizophoraceae develop from fruit to seedling (*i.e.* the dispersal unit or propagule) without a dormancy period when still attached to the parent tree (Tomlinson 1994). Lateral roots already appear early during seedling development, and are visible as bumps on the outside of the seedling tip (Juncosa 1982a). As an adaptation to the mangrove environment, in which tides that inundate the forest at regular times are responsible for dispersal, abscised seedlings have an initial ability to float (Rabinowitz 1978; Tomlinson 1994). Their anatomy is thus different from that of other young trees. Mangrove seedlings primarily consist of an elongated and thickened cylinder-shaped structure, the hypocotyl, topped by a short embryonic shoot (plumule) (Sousa *et al.* 2007) consisting of the growing epicotyl and first leaf pair (Raven *et al.* 2005) (Fig. 1A). The hypocotyl contains a high amount of air-filled intercellular spaces (aerenchyma) in between the cortex parenchyma that help the seedlings to float (Tomlinson 1994; De Ryck 2009). Once stranded, they must establish quickly and firmly, mobilise nutrients and organic compounds stored in their hypocotyl (Smith & Snedaker 2000) and outgrow the tidal reach. The vascular tissue is already present since the early development of the seedlings on the parent tree (N. Tonné – personal observation), allowing direct water and nutrient uptake when properly established.

Upon establishment, the present anatomical tissues and structures allow mangrove seedlings to cope with frequent flooding by seawater (Youssef & Saenger 1996). The cortex of rhizophoraceous mangrove seedlings can be divided into two zones, the outer and the inner cortex (Juncosa 1982b), and is aerenchymatous in varying degrees depending on the species (Juncosa 1982b; Tomlinson 1994). In most cases the inner layers of the cortex are more aerenchymatous than the somewhat more compact and thicker-walled outer cortex layers (Tomlinson & Cox 2000). Also the pith tissue has been observed to be aerenchymatous in *Rhizophora mangle* (Juncosa 1982a) (without a connection between the pith aerenchyma and the atmosphere during the floating stages). It resembles the outer cortex anatomically in some *Bruguiera* species (Juncosa 1982b). The aerenchyma in the ground tissue enables mangrove seedlings to float and to conserve oxygen for aerobic metabolism when flooded (Youssef & Saenger 1996). Both pith and cortex are known to function as storage tissues (Eames & MacDaniels 1947), showing abundant starch content in mangrove hypocotyls (Juncosa 1982b). Lenticels on the surface of the hypocotyls of some species facilitate gas exchange to the underlying cortex (Tomlinson 1994).

In *Rhizophora mangle* the parent tree transports water and nutrients to its attached embryos/seedlings via specialised transfer structures present in both parental and embryo/seedling tissues (Wise & Juncosa 1989). Tomlinson and Cox (2000) and Fisher and Tomlinson (2002) observed that the rooted distal end of horizontally stranded *R. mangle* and *Bruguiera gymnorrhiza* seedlings bends when the hypocotyl elevates from the ground. The distal end thereby forms a hook, and gelatinous (or tension wood)

fibres produced on the upper side of the hook are likely the cause of bending. Cheeseman (2012) additionally observed that *R. mangle* seedlings alternately elevate and relax in a diurnal cycle during self-elevation, that they develop an upward curvature in the hypocotyl, and that the epicotyl swells in a later stage. This is followed by the first leaves that unfold before the seedling is fully elevated. Yet, surprisingly enough, not much more has been published about the anatomy of developing mangrove trees in their early life stages, though it is crucial for their ecological and biogeographical success (Spalding *et al.* 2010).

To fill this knowledge gap, we studied the change in anatomy of mangrove seedlings over time by combining two different visualisation techniques: a non-destructive (X-ray Computed Tomography - CT) and a destructive method (light microscopy of microtome sections). With X-ray CT it is possible to acquire a continuous series of two-dimensional density images through an object in a non-invasive way (Castell *et al.* 2005; Buzug 2008; Van den Bulcke *et al.* 2009; Brodersen *et al.* 2011; Brodersen 2013). These images then can be combined to obtain a full three-dimensional picture of the object in all directions. X-ray CT has many applications in wood research, *e.g.* in wood degradation using density maps (Hervé *et al.* 2014), for tree growth rings in dendroclimatological research (Dutilleul *et al.* 2014), to determine the water distribution in sapwood and heartwood of the stem as well as in earlywood and latewood of an annual ring (Fromm *et al.* 2001), and for density profiles of wood cores (De Ridder *et al.* 2011). However, to our knowledge, X-ray CT has not yet been used to study internal plant development over time in young trees or herbaceous plant species, let alone in combination with light microscopy.

For this paper two mangrove species were studied, *Bruguiera gymnorrhiza* and *Ceriops tagal*, in their first development stages after establishment. In a first step, we made an anatomical description of the various hypocotyl tissues present in both species based on light microscopy of microtome sections and established the link between the sections and the images obtained by CT-scanning. Next, we used X-ray CT to follow two plants, one per species, over a period of fourteen months when developing an epicotyl with leaves*), and completed this analysis with light microscopy of sections of young plants of the same species that were one month to one and a half year old. Our goal was to investigate the variation in hypocotyl tissue proportions (i) over time during the development from seedling to young plant and (ii) with hypocotyl height, based on the combination of the two aforementioned visualisation methods. Four main hypotheses were posited:

1) the vascular tissue would proportionally increase over time in both species as its importance grows;
2) accompanied by proportional decreases in the other hypocotyl tissues;
3) the proportions of all hypocotyl tissues would remain constant throughout the analysed length of the hypocotyl during development;
4) the two different visualisation techniques in the developmental study of mangrove seedling would provide a more complete picture of their development than only one technique.

*) See also Supplementary Table 1 in de online edition of this journal, which can be accessed via http://booksandjournals.brillonline.com/content/journals/22941932.

MATERIALS AND METHODS

Plant material

This study was conducted on mangrove seedlings – *i.e.* mangrove plants smaller than one metre (Krauss *et al.* 2008) – of two mangrove species: *Bruguiera gymnorrhiza* (L.) Sav. and *Ceriops tagal* (Perr.) C.B. Rob. Propagules were collected in January 2013 in the mangrove forest of Mida Creek in the Watamu Marine National Reserve, located 88 km north of Mombasa and in February 2013 in Gazi Bay, approximately 50 km south of Mombasa on the Kenyan coast. Both mangrove forests are comparable due to a similar mangrove zonation pattern, the type of mangrove forest they constitute (*i.e.* a fringing mangrove forest), and the fact that both forests are connected to the Indian Ocean (*i.e.* Mida Creek has a narrow opening towards the ocean, and Gazi Bay is widely open to the ocean) (Dahdouh-Guebas *et al.* 2002). In addition, both areas have a tidal regime that is general along the East-African coast, with a semi-diurnal periodicity having a mean variation in tidal amplitude of 2.5 to 3 m (Obura 2001). As such, the plants analysed in our study had a comparable ecological background when sampled.

In order to collect ripe propagules, parent trees were gently shaken and fallen propagules were collected. The propagules were immediately transported to Belgium, potted upon arrival in a mixture of potting soil, loam and sand (1 : 1 : 1 ratio) and maintained in brackish water (15‰ NaCl) within a greenhouse (standardised conditions: air temperature: 20 °C at night and 25–30 °C during the day; relative air humidity: 70 %; light: 100 µmol photons $m^{-2}*s^{-1}$; day-night cycle during the autumn and winter months: 12 : 12; natural light during the spring and summer months). The plants were sprayed daily with fresh water. One *B. gymnorrhiza* plant was kept in water with a salinity of 33‰ during a floating experiment, and potted afterwards on 12 April 2013.

CT-analysis

One young plant of each species was scanned every two to three weeks from 6 March 2013 until 9 October 2013 and once on 28 May 2014, using a multi-slice spiral CT-scanner (Brilliance CT 64-channel scanner, Philips, The Netherlands). The following scanning settings were used: collimation: 20 × 0.625 mm; slice thickness: 0.67 mm; reconstructed slice interval: 0.33 mm; fixed tube current and power (350 mAs and 140 kV); X-tube rotation time: 0.75 s; reconstruction filter: Y-sharp (YE). The field of view was adapted to the size of each scanned object. Images were reconstructed in an axial plane with a high resolution 768 × 768 matrix. On the axial 50 % overlapping image stack, radial and three-dimensional reconstructions were made on a dedicated Philips CT workstation (Extended Brilliance Workspace, Philips, The Netherlands).

Due to the interference of the potting soil with the X-rays of the CT-scanner, only the aboveground part of the seedlings could be analysed. We selected five heights for analyses: 0 % (*i.e.* the height right above the soil), 20 %, 50 % and 80 % of the length of the aboveground part of the plant and 100 % (*i.e.* the height immediately below the epicotyl) (Fig. 1A). Per height, five images were analysed equally distributed within a zone of approximately 2 mm. The area of each of the tissues was measured in Photoshop (Adobe Photoshop CS5 Extended, version 12.0 × 32, San José, California, USA), after which the average, minimum and maximum proportions of each tissue were calculated.

Based on longitudinal CT-images from 9 October 2013 through the hypocotyl of both seedlings, a longitudinal density profile of the pith along the length of the hypocotyl was derived from height one to five (Fig. 1A) with a spatial frequency of one millimetre. For each slice, the average CT-value was obtained in a segmented region of interest (ROI) that represented the cross section of the pith. Image segmentation was done with open source software for medical image processing (Fedorov *et al.* 2012). The obtained CT-value profile reflects the longitudinal change in average material density – measured by X-ray attenuation – of the pith along the hypocotyl starting from height one to height five. In X-ray imaging, the density of a tissue can be characterised by its linear attenuation coefficient µ(E) which, in CT-imaging, is expressed by CT-values in Hounsfield Units (HU). HUs are relative values of X-ray attenuation in an object with the density of water as a point of reference (HU = 0). Tissues with an attenuation lower or higher than that of water, will have negative or positive HU-values respectively. The density of a tissue is also illustrated by the white-to-black colour scale of its CT-image, with the scale representing a decrease in tissue density from white to black. Analogously, a longitudinal density profile of all tissues together was taken for both species, also from hypocotyl height one to five.

Light microscopy analysis

We sampled mangrove seedlings of both *B. gymnorrhiza* and *C. tagal*, which were potted in January or February 2013 (for the timing of sampling, see Fig. 1B). Before sampling, we measured the total hypocotyl length of the seedlings and counted the total number of leaves. Hypocotyl mid-height (*i.e.* at 50 % of the total hypocotyl length) samples were made and preserved in a Copenhagen mixture (70 % ethanol, glycerol and demineralised water – ratio: 1 : 1 : 1) until sectioning. Transverse sections of 15–25 µm were made of the hypocotyl samples using a sliding microtome (Sledge GSL1, Zürich, Switzerland (Gärtner *et al.* 2014)). These sections were put on a labelled microscope slide and bleached with sodium hypochlorite ('Eau de Javel') for a few minutes in order to remove the phenols (Gärtner & Schweingruber 2013), and subsequently rinsed well with demineralised water. They were stained with a mixture of safranin O (0.35 g in 35 ml of 50 % ethanol) and alcian blue (0.65 g in 65 ml water) for circa one minute. Surplus stain was removed with demineralised water before the sections were dehydrated by successively rinsing them with 50 %, 75 % and 96 % ethanol. Finally, they were embedded with a few drops of Canada balsam, covered with a cover glass and dried overnight in an oven at 60 °C.

Pictures of the sections were made with a camera connected to a microscope (Olympus UC30 and Olympus BX60 respectively, Olympus Europa Holding GmbH, Hamburg, Germany), using the image analysis software programme Cell^B (Olympus Europa Holding GmbH, Hamburg, Germany). Afterwards, we connected the images together by means of the panoramic stitching software PTGui (New House Internet Services BV, Rotterdam, The Netherlands), in order to analyse them in Photoshop as described for the CT-images.

Per species, multiple linear regression was performed on the data of each tissue. When data were not normally distributed, they were log-transformed first. All statistics were executed in STATISTICA 8.0 (StatSoft Inc., Tulsa, USA).

CT- and light microscopy image comparison

In order to identify the hypocotyl tissues on the CT-images, we analysed the overlap between a CT-image and a section of the same plant. Hence, one seedling of *B. gymnorrhiza* and one of *C. tagal* were CT-scanned in accordance with the abovementioned procedure. The *B. gymnorrhiza* seedling was potted in January 2013, and the *C. tagal* seedling in February 2013. The seedlings were CT-scanned on 17 June 2014 and 20 August 2014 respectively, and mid-height hypocotyl samples were immediately taken the same day. Of these samples, transverse sections were made and analysed as described above ('*Light microscopy analysis*'). In addition, these sections were compared with the corresponding CT-images of the hypocotyl at the same height in order to establish the anatomical link between both kinds of images.

RESULTS AND DISCUSSION

Anatomical observations

The different mangrove seedling hypocotyl tissues (cortex, vascular tissue and pith) were clearly recognizable on the CT-images. They could easily be identified through a single comparison of CT-images and sections of the scanned and subsequently sampled *Bruguiera gymnorrhiza* and *Ceriops tagal* seedlings (Fig. 2A1 & B1). This confirmed that CT-images can be used for the identification and delineation of different anatomical tissues (in young plants), which become visible and distinguishable based on tissue density differences.

In the sections we observed that the cuticle layer was thick in both species, but it was thickest in *C. tagal*, according to Juncosa (1982b) the thickest of the tribe Rhizophorae. The epidermis had a single layer of radially elongated cells in both *B. gymnorrhiza* and *C. tagal* (Fig. 2A7 & B7) ("giving the epidermis a palisade-like appearance" as phrased by Wilkinson (1981)), which were shorter in *B. gymnorrhiza*. In both species we observed cork (phellem) cells at some places beneath the epidermis at this stage (*i.e.* seedlings between 430 and 551 days old), as well as phelloderm cells in *C. tagal* (Fig. 2A7 & B7). A transition from round and compactly arranged cells to loosely arranged roundish and radially elongated cells could be observed from the outside to the inside of the cortex in both species (Fig. 2A3 & A4, B3 & B4). This kind of cortical cellular gradient has also been found in other rhizophoraceous mangrove species such as *Bruguiera exaristata*, *B. parviflora* (Juncosa 1982b) and *Rhizophora mucronata* (Bobda *et al.* 2015). The loosely arranged inner part of the cortex of both species contained a mix of thin- and thicker-walled cells. In the longitudinal direction (confirmed by longitudinal sections), the inner cortex zone cells could be roundish as well as longitudinally elongated, and some cells had unevenly thickened and lignified cell walls. At the boundary of the inner cortex and the vascular tissue in both species, a thin-walled endodermis was present with a conspicuous Casparian strip (Fig. 2A5 & B5). The vascular tissue consisted of a ring of united vascular bundles (the bundles

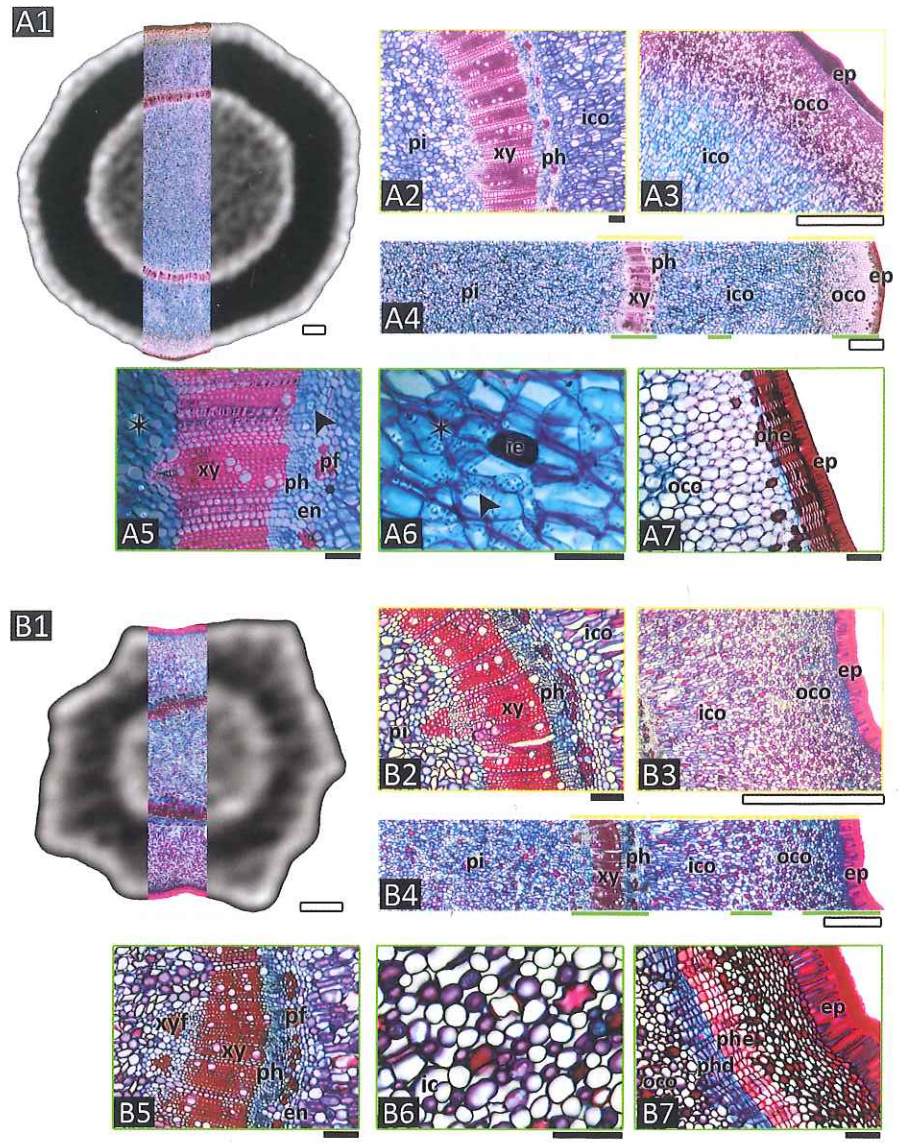

Figure 2. – A1 and B1: CT-image and corresponding section, both at hypocotyl mid-height of a scanned and subsequently sectioned 430-days-old *Bruguiera gymnorrhiza* seedling (A1) and a 551-days-old *Ceriops tagal* seedling (B1). The white-to-black scale of the CT-images indicates dense to less-dense tissues respectively. – A2 to A7: Transverse sections of the *B. gymnorrhiza* seedling at hypocotyl mid-height showing the different tissues in detail. Figures A5 and A6 were taken under polarised light. – B2 to B7: Transverse sections of the *C. tagal* seedling at hypocotyl mid-height showing the different tissues in detail. The colours of the sections refer to unlignified cells (blue – Alcian Blue) and lignified cells or phenolic substances (red – Safranin O). Scale bars represent 1 mm (white bars) or 100 μm (black bars). – en: endodermis; ep: epidermis; ic: intercellular cavity (air space); ie: secretory idioblast (oil cell); ico: inner cortex; oco: outer cortex zone; ph: phloem; phd: phelloderm; phe: phellem; pi: pith; pf: pericyclic fibres; st: starch; xy: xylem; xyf: xylem fibres; arrowhead: crystal druse; star: starch grains.

united with time during seedling growth) containing the usual xylem and phloem tissues with their typical cell types found in eudicot plants (Fig. 2A2 & A5, B2 & B5). In the early stages in both species, not all vascular bundles contained xylem elements, as was also observed in *C. tagal* by Wilkinson (1981). In longitudinal view, we noted that the vessel elements contained scalariform perforation plates containing less than 10 bars and horizontal scalariform intervessel pits (confirmed by InsideWood 2004-onwards). Fibres on the inside of the vascular bundles (bundle sheath or xylem fibres (Tomlinson & Cox 2000)) were observed in *C. tagal* (Fig. 2B5). On the outside of the vascular bundles highly lignified pericyclic or phloem fibres (Tomlinson & Cox 2000) were discerned in both species (Fig. 2A5 & B5), but they were more conspicuous in *C. tagal* than in *B. gymnorrhiza*. In the seedlings of the latter, these pericyclic fibres developed in a later stage as they were not observed in sections of the youngest *B. gymnorrhiza* seedlings as also stated by Metcalfe and Chalk (1957). The pith tissue contained roundish thin-walled cells in both species (Fig. 2A2 & B2). Yet, in *C. tagal* thicker-walled cells with an unevenly thickened lignified cell wall were present too, which could be roundish in all directions or longitudinally elongated (confirmed by longitudinal sections) (Fig. 2B2 & B5).

The pith as well as the cortex store abundant starch grains and thereby serve as storage tissues (Tomlinson & Cox 2000; Evert 2006) that are exploited during the development of the mangrove seedlings (Smith & Snedaker 2000). In the sections of these seedlings starch has only been observed in the cortex (more frequently in the inner than in the outer cortex zone) and pith tissues of *B. gymnorrhiza* (Fig. 2A5 & A6) but not anymore in the tissues of *C. tagal*. The cortex in addition serves as a protective tissue and provides mechanical support (Eames & MacDaniels 1947). Secretory idioblasts containing oil or tannins (Foster 1956) were distinguished in the cortex (mainly inner zone) and pith of *B. gymnorrhiza* (Fig. 2A6) and *C. tagal*. Intercellular air spaces were observed in the inner zone of the cortex and the pith of both species, where the pith was more compact than the inner cortex. Equally found in the cortex and pith of both species were cells containing druse crystals, as well as in the phloem tissue of *B. gymnorrhiza* (Fig. 2A5 & A6).

On the CT-images, the vascular tissue zone appeared white indicating its high density which was caused by the presence of dense lignin (Stamm & Hansen 1937) in the thickened walls of cells such as xylem vessel elements, fibres, and sclereids. Also the outer zone of the cortex was identified as a dense tissue on the CT-images. The pith and the inner zone of the cortex on the other hand appeared grey or black, which indicated that these tissues primarily consisted of cells containing non-lignified cell walls (Evert 2006), as observed in the sections, creating a non-dense tissue. The transition between the inner and outer cortex zones, which was indicated by the density transition from white to grey or black on the CT-images, was gradual in *C. tagal* and less so in *B. gymnorrhiza*. Likewise there was a transition in cell shape from the outer to the inner cortex in the sections, which was more gradual than the white-grey/black density transition on the CT-images. The two cortex zones were analysed together, as the proportional trends of the separate zones coincided with that for the cortex tissue as a whole (data not shown). Especially the inner cortex contributed to the trend observed for the whole cortex.

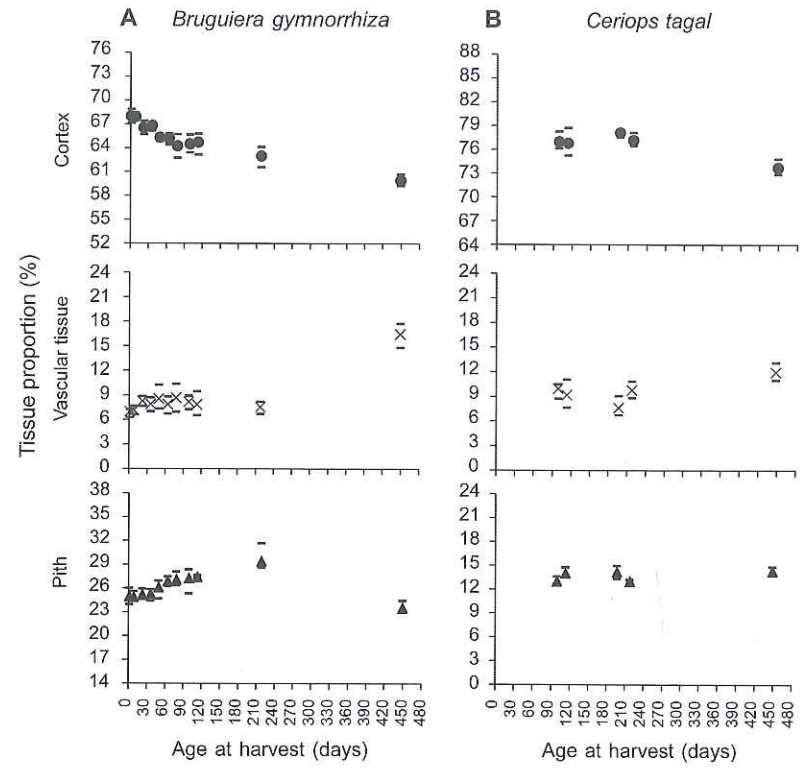

Figure 3. Average proportions of the different hypocotyl tissues (cortex, vascular tissue and pith) over time for *Bruguiera gymnorrhiza* (A) and *Ceriops tagal* (B), with the corresponding minimum and maximum values. Time = 0 days corresponds to the date the seedlings were scanned for the first time, which is the same for both species. The graphs represent the average tissue proportions for aboveground hypocotyl height 2 (Fig. 1A), which is mid-height of the hypocotyl and therefore corresponds to the sections made of the mid-height samples (*i.e.* 50 % of the total hypocotyl length) in the harvested seedlings.

Anatomy of young developing mangrove seedlings over time

Both visualisation techniques, non-destructive CT-scanning of whole young plants and light microscopy of destructive sections of hypocotyl mid-height samples, confirmed that the vascular tissue of *B. gymnorrhiza* and *C. tagal* seedlings proportionally increased over time (as well as in absolute area – data not shown) (Fig. 3*) (multiple linear regression on the data of the hypocotyl mid-height sections: *B. gymnorrhiza* - $F = 64.27$, $p < 0.001$, $R^2 = 0.75$; *C. tagal* - $F = 85.61$, $p < 0.001$, $R^2 = 0.83$) (Fig. 4). The same trend could also be distinguished at the other hypocotyl heights in both species (Fig. 5). This underlines the growing importance of the vascular tissue over time in the development of the young mangrove seedlings, as stated in our first hypothesis.

*) See also Supplementary Table 2 in de online edition of this journal, which can be accessed via http://booksandjournals.brillonline.com/content/journals/22941932.

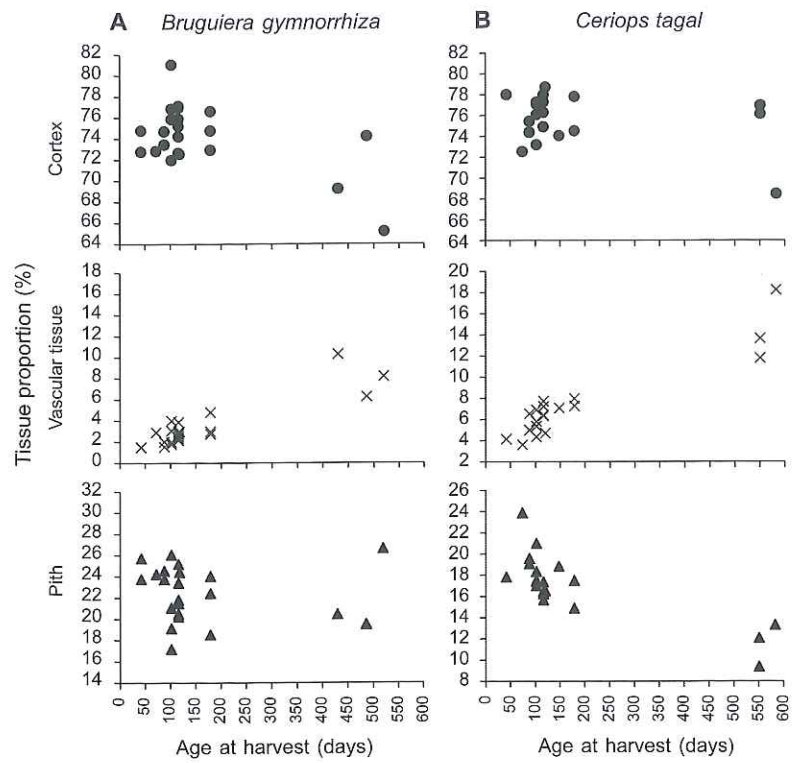

Figure 4. The tissue proportions in function of age at harvest, measured in the sections of the hypocotyl mid-height samples of the harvested *Bruguiera gymnorrhiza* (A) and *Ceriops tagal* (B) seedlings (Fig. 1B).

The proportional change in vascular tissue was accompanied by changes in the relative proportions of the other hypocotyl tissues in both species. Via CT-analysis we observed that the cortex tissue at hypocotyl mid-height proportionally decreased over time in *B. gymnorrhiza* and *C. tagal* (Fig. 3A & B). These results were in accordance with the results of the hypocotyl mid-height sections, although non-significant for *C. tagal* (multiple linear regression: *B. gymnorrhiza* - $F = 4.85$, $p < 0.05$, $R^2 = 0.19$; *C. tagal* - $F = 1.95$, $p = 0.18$, $R^2 = 0.10$) (Fig. 4A & B). The abovementioned CT-analysis trends equally held for the other hypocotyl heights in case of *B. gymnorrhiza*, and for most of the other heights in *C. tagal*. The proportional cortex decrease was in line with our second hypothesis, stating that it would accompany the proportional increase in the vascular tissue over time. In the first stages of seedling development, these decreases were also likely linked with the role of the cortex in providing the developing seedlings with starch. The stored reserves are exhausted early in mangrove seedling development (Smith & Snedaker 2000), as was noted in the sections of *C. tagal* (see anatomical description).

The pith tissue in *B. gymnorrhiza* proportionally increased at hypocotyl mid-height in the beginning of the experiment, but once the vascular tissue started to proportionally increase (Fig. 3A, after c. 210 days) the pith proportionally decreased. This pattern could also be discerned at most of the other hypocotyl heights (Fig. 5A*). The light microscopy study, however, indicated a non-significant decreasing linear trend ($F = 0.87$, $p = 0.36$, $R^2 = 0.04$) (Fig. 4A). In *C. tagal* the average pith proportion mainly remained stable (or slightly increased) over time at all hypocotyl heights (Fig. 5B*), whereas it significantly decreased ($F = 29.42$, $p < 0.001$, $R^2 = 0.62$) according to the light microscopy study (Fig. 4B). The conflicting results of the CT- and light microscopy analysis for the pith tissue in both species do not allow for a conclusive answer regarding its development over time. Hence the second hypothesis remains unresolved regarding the pith tissue. We think these discrepancies are a consequence of the limited sample size in combination with biological variation between individuals, which must be resolved by scanning and sectioning more individuals per species.

Not many studies that include quantification of the various stem tissue proportions of young plants in general were found. Older surveys state that the final diameter of the pith in a dicotyledonous (eudicot) stem is reached early in development (Eames & MacDaniels 1947; Marcelis-van Acker 1994) resulting in a constant pith area along the plant's stem (Lauri *et al.* 2011). Hence, in most woody species the pith makes up only a small part of the total cross-sectional area of the stem (Metcalfe & Chalk 1979). We also observed that the absolute area of the pith remained stable over time in *B. gymnorrhiza*, and the same could be discerned when examining the cortex and pith in *C. tagal* (data not shown). However, slight increases in absolute area of the cortex at hypocotyl heights one and five in *B. gymnorrhiza* were in fact found (data not shown). When a seedling develops it relies increasingly on its vascular tissues for water and nutrient transport, structure and mechanical support, and less on carbon storage tissues such as the cortex. Yet, more research on the function of non-lignified tissues in plant development and the variation or patterns herein in relation to (varying) environmental factors is needed to understand the roles of these tissues and their importance in plant growth. Mangrove seedlings offer a very particular case in anatomy, related to their adaptive function in the intertidal environment.

Anatomy of young developing mangrove seedlings with height position in the hypocotyl

The average proportions of the tissues in the CT-scanned seedlings did not only vary over time, but also with hypocotyl height (Fig. 1A*). The vascular tissue proportionally increased and the cortex proportionally decreased with height in both species, and these trends persisted throughout the experiment*). In other words, near the epicotyl there was proportionally more vascular and less cortex tissue than lower in the hypocotyl. This observation was not in line with our third hypothesis. It could be explained by the functional roles of the vascular tissue and cortex in a plant stem or similarly, in a mangrove seedling hypocotyl. At the roots or the lowest tip of a mangrove seedling hypocotyl living cells, such as in the cortex, play a considerable role in processes of water and nutrient uptake and root production. Higher in the hypocotyl the vascular

*) See also Supplementary Table 2 in de online edition of this journal, which can be accessed via http://booksandjournals.brillonline.com/content/journals/22941932.

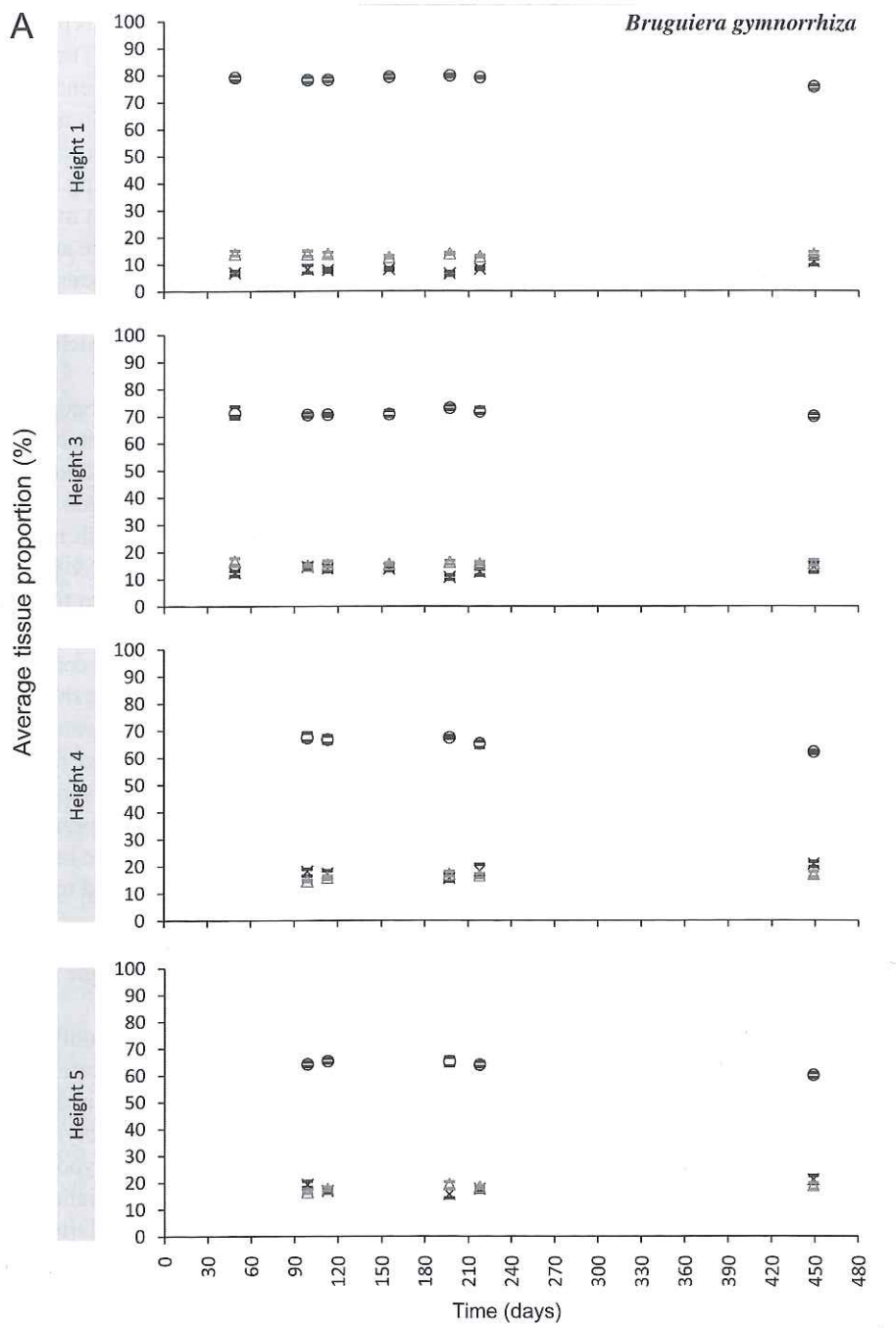

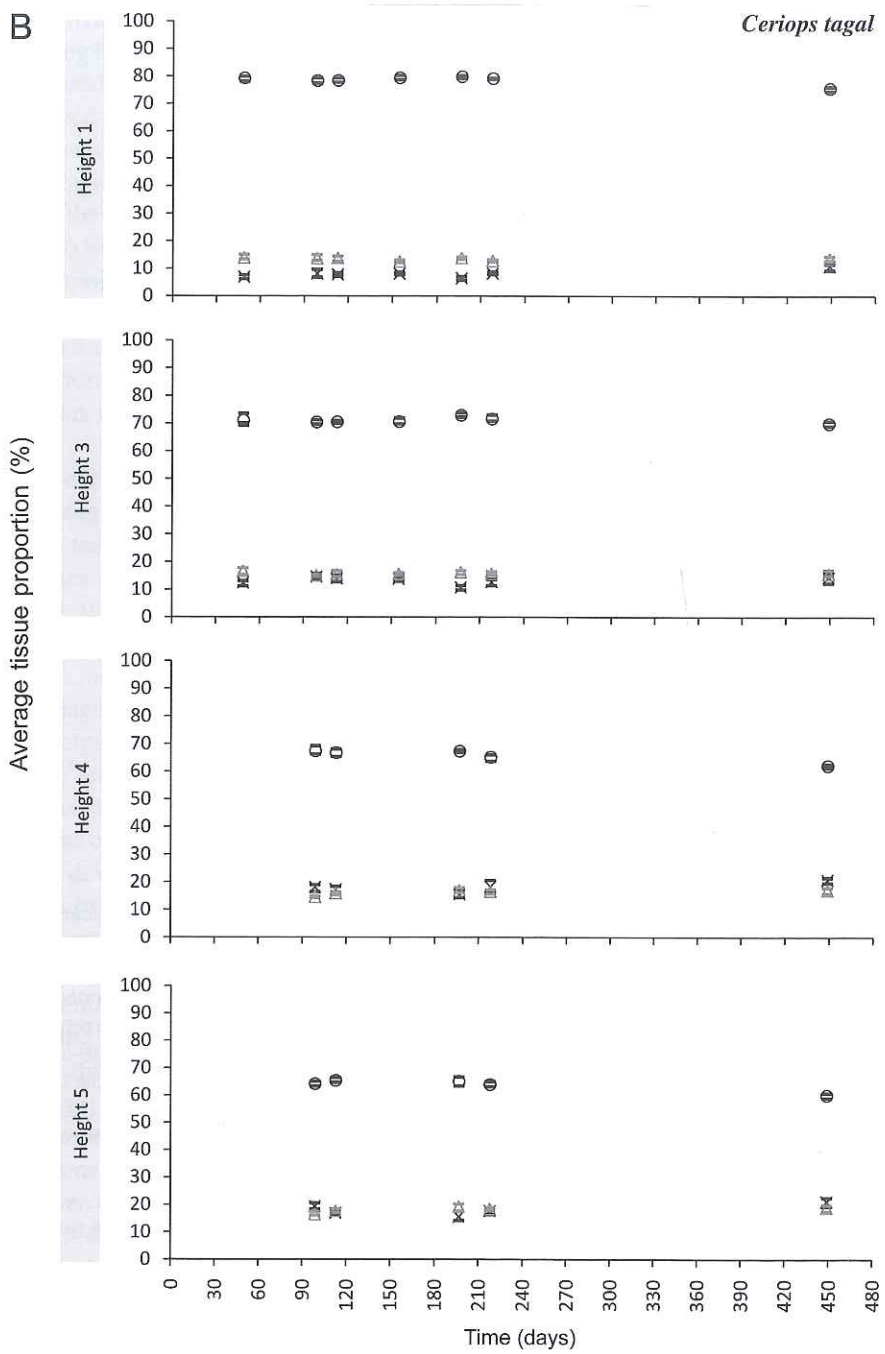

Figure 5. The average proportions of the various hypocotyl tissues over time for *Bruguiera gymnorrhiza* (A, above) and *Ceriops tagal* (B, next page), for hypocotyl heights one and three to five. — ○ = cortex; × = vascular tissue; △ = pith; ━ = min and max.

○ = cortex; × = vascular tissue; △ = pith; ━ = min and max.

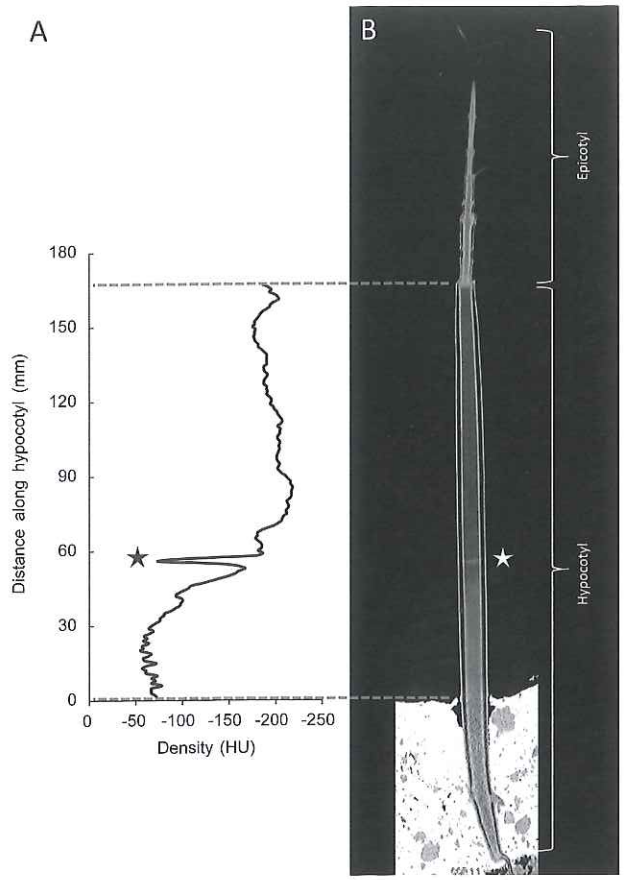

Figure 6. A CT-image through the hypocotyl of the *Bruguiera gymnorrhiza* seedling scanned on 9 October 2013 (B), with a longitudinal density profile of the pith along the length of the hypocotyl (A). The longitudinal density profile reflects the average CT-value in Hounsfield Units (HU) of the pith along the hypocotyl from height one to height five. The pith is illustrated as the central tissue cylinder of the hypocotyl. The HU-scale ranging from zero to negative represents a decrease in density. Analogously, the density of the tissue is illustrated by the white-to-black scale of the CT-image, representing a decrease in density from white or light grey to darker grey or black. The sudden increase in the HU-value around 60 mm along the hypocotyl (black star in A) is an image artefact created by a metal wire that was attached to the pot of the seedling interfering with the X-ray radiation (white star in B).

tissue becomes more important than the cortex, because of its role in passing on water and nutrients to neighbouring cells and the growing epicotyl and leaves.

The pith tissue proportionally increased with height in both species. This trend persisted in *C. tagal*, but not in *B. gymnorrhiza* *). As for the vascular and cortex tissues, these trends were not in line with our third hypothesis.

*) See also Supplementary Table 2 in de online edition of this journal, which can be accessed via http://booksandjournals.brillonline.com/content/journals/22941932.

From the longitudinal density profiles of the pith in the *B. gymnorrhiza* and *C. tagal* seedling hypocotyls scanned on 9 October 2013, it was clear that the density of the pith decreased from the soil surface towards the epicotyl (Fig. 6). The same pattern could be observed from a longitudinal density profile of all tissues together (data not shown). In other words, the seedlings were denser in their hypocotyl near the soil than higher up near the epicotyl. Mangrove seedlings, colonizing and thriving in the intertidal areas along the tropical and subtropical coasts which form a highly dynamic environment, need to withstand tidal and wind action and water currents. Certainly during the early development stages, when they are unstable and fragile and must develop a large rooting anchor, being denser at the base could offer support against action of tides and wind (Balke *et al.* 2011). The pith (as well as the cortex) is known to serve besides food storage also water storage in plant stems. Our observations on the pith suggest a complex role of ground tissues in mangrove seedlings.

Comparison of the different visualisation techniques – light microscopy and CT-scanning

We tested and experienced the combination of CT-analyses with light microscopy analyses on sections as a useful approach in the anatomical study of young mangrove plants, which confirms our fourth hypothesis. Light microscopy allowed detailed anatomical observations at cell level and/or tissue level which are not possible on CT-images, and thereby helped in the identification of the different tissues revealed by the CT-images. Once the anatomical link between both kinds of images was established, CT-scanning could be easily applied in the study of young plant development with a high temporal resolution. Medical CT-scanners are designed to produce detailed 3D images of biomedical materials in large objects at a very high speed during which they can cover large volumes. This makes them particularly suitable in the investigation of the development of whole young (mangrove) plants. Additionally, thanks to their non-destructiveness it becomes possible and easy to investigate intact young developing plants over a longer time-period at the tissue level without the need to kill the plant (Brodersen 2013; Metzner *et al.* 2015; Subramanian *et al.* 2015).

Opening up possibilities in regions where mangroves as well as hospitals with CT-scanning facilities occur, would allow the application of CT-scanning techniques in unravelling the internal development over time in a wide range of mangrove species seedlings. We are confident that CT-scanning can also be used in the study of non-mangrove plant seedlings as well as older plants, both regarding their development over time and their anatomy.

When examining young plants, one has to take into account that there is a sufficient amount of differences in X-ray attenuation present between the various tissues to be observed. When the attenuation of adjacent tissues is too similar, for example due to homogeneous densities, the image contrast between those tissues on the CT-image is reduced. This can be the result of a high moisture content in the tissues (Espinoza *et al.* 2005; Witomski *et al.* 2010), which might be the case in young mangrove plants (Lechthaler *et al.*, submitted), and/or the fact that young plants do not yet contain much lignified tissue which contributes to tissue density and, hence, image contrast.

In addition, those hypocotyl heights were located right above the soil (mixture of potting soil, sand and loam) which tends to interfere with X-rays, adding to the reduced image contrast. In this study, the analysis of *C. tagal* therefore started later than that of *B. gymnorrhiza* (23 April / 12 June 2013 compared to 6 March 2013) once the plant had developed a sufficient amount of density differences between its various tissues. The above-mentioned factors were also present in the *B. gymnorrhiza* seedling but to a lesser extent. This is probably because *B. gymnorrhiza* seedlings have a thicker hypocotyl (Tomlinson & Cox 2000) and thus more volume and a higher initial amount of lignified tissue that can counteract X-ray interfering effects from factors such as potting soil. In addition, a higher amount of lignified tissue improved the image contrast on the CT-image and hence did not trouble CT-image analysis.

CONCLUSIONS

To our knowledge, the internal development of young plants over time has not yet been studied extensively and thus remains an interesting field in plant anatomy to be further explored. In this regard, CT-scanning is a promising technique as it allows investigating plants internally *in vivo* in a non-destructive manner. Moreover, light microscopy observations of sections of plant samples allow studying stem or hypocotyl tissues at cell level resolution. The combination of both techniques contributes to a more complete picture of the internal development of young plants and is applicable on a wide range of plant species.

Both mangrove seedlings have homologous structures as they belong to closely related genera within the tribe Rhizophorae (Shi *et al.* 2002) of the family Rhizophoraceae. Yet, the results of our study suggest that, apart from the vascular tissue, there is no uniform way of mangrove hypocotyl tissues to develop both over time and with hypocotyl height. In fact, there is variation both within and between species and more data will help to clarify the observed trends. In addition, we observed that all hypocotyl tissue proportions changed faster over time in *Bruguiera gymnorrhiza* than in *Ceriops tagal*, which is probably a consequence of the slower growth of the latter species (Kairo 1995; Duke *et al.* 2010).

Both species occur in different positions on the tidal flat (Matthijs *et al.* 1999), thus a next step in the enlargement of the dataset could be to take the effect of environmental conditions on the internal development of young plants experimentally into account. This is especially important in the mangrove forest, where the environmental conditions are physically and physiologically challenging for plants and change very rapidly over time and space (short distances). What's more, physiological processes in all other plant organs – such as the leaves and epicotyl – in relation to local environmental conditions should be addressed as well. Only this integrated approach will lead to an understanding of mangrove seedling survival, which is important for mangrove forest regeneration and restoration.

ACKNOWLEDGEMENTS

The authors are grateful to Mohamed Omar Said Mohamed of Kenya Wildlife Service (KWS, Kenya) and to James Gitundu Kairo of the Kenya Marine and Fisheries Research Institute (KMFRI, Mombasa, Kenya) for collection of mangrove propagules, and to Martine Claeys for her help in the greenhouse.

The study was financially supported by the Research Foundation - Flanders (FWO, Flanders, Belgium). We thank the Department of Radiology of the Universitair Ziekenhuis Brussel for offering free CT-scanning, and Maarten De Munter for executing the CT-scans. We also thank Alan Crivellaro for offering his help on the microtome sectioning. We are grateful to the two anonymous reviewers for their comments on an earlier version of this paper. This research is published within the framework of the EC-funded Marie-Curie International Research Staff exchange Scheme entitled Coastal Research Network on Environmental Changes - CREC (Grant Agreement nº 247514) and is linked to activities conducted within the COST FP1106 network.

REFERENCES

Balke T, Bouma TJ, Horstman EM, Webb EL, Erftemeijer PLA & Herman PMJ. 2011. Windows of opportunity: thresholds to mangrove seedling establishment on tidal flats. Marine Ecology Progress Series 440: 1–9.

Bobda RM, Pandey R & Pandey CN. 2015. Histological findings in hypocotyl of *Rhizophora mucronata* Lamk. (Rhizophoraceae family). Internat. Sci. J. 1: 20–27.

Brodersen CR. 2013. Visualizing wood anatomy in three dimensions with high-resolution X-ray micro-tomography (μCT) – a review. IAWA J. 34: 408–424.

Brodersen CR, Lee EF, Choat B, Jansen S, Phillips RJ, Shackel KA, McElrone AJ & Matthews MA. 2011. Automated analysis of three-dimensional xylem networks using high-resolution Computed Tomography. The New Phytologist 191: 1168–1179.

Buzug TM. 2008. Computed Tomography. From photon statistics to modern cone-beam CT. Springer-Verlag, Berlin, Heidelberg.

Castell WZ, Schrödl S & Seifert T. 2005. Volume interpolation of CT images from tree trunks. Plant Biology 7: 737–744.

Cheeseman JM. 2012. How red mangrove seedlings stand up. Plant Soil 355: 395–406.

Dahdouh-Guebas F, Vermeirt M, Cannicci S, Tack JF & Koedam N. 2002. An exploratory study on grapsid crab zonation in Kenyan mangroves. Wetl. Ecol. Manag. 10: 179–187.

De Ridder M, Van den Bulcke J, Vansteenkiste D, Van Loo D, Dierick M, Masschaele B, De Witte Y, Mannes D, Lehmann E, Beeckman H, Van Hoorebeke L & Van Acker J. 2011. High-resolution proxies for wood density variations in *Terminalia superba*. Ann. Bot. 107: 293–302.

De Ryck D. 2009. Moving and Settling: Experiments on the dispersal and establishment of hydrochorous propagules. Department of Biology, Vrije Universiteit Brussel.

Duke N, Kathiresan K, Salmo IS, Fernando E, Peras J, Sukardjo S & Miyagi T. 2010. "*Ceriops tagal*". http://www.iucnredlist.org. Downloaded on 19 August 2015.

Dutilleul P, Han LW & Beaulieu J. 2014. How do trees grow? Response from the graphical and quantitative analyses of computed tomography scanning data collected on stem sections. Comptes rendus biologies 337: 391–398.

Eames AJ & MacDaniels LH. 1947. An introduction to plant anatomy. McGraw-Hill Book Company, Inc., New York, London.

Espinoza G, Hernandez R, Condal A, Verret D & Beauregard R. 2005. Exploration of the physical properties of internal characteristics of sugar maple logs and relationships with CT images. Wood Fiber Sci. 37: 591–604.

Evert RF. 2006. Esau's Plant Anatomy. Meristems, cells, and tissues of the plant body: their structure, function and development. Wiley & Sons, Inc., New Jersey.

Fedorov A, Beichel R, Kalpathy-Cramer J, Finet J, Fillion-Robin J-C, Pujol S, Bauer C, Jennings D, Fennessy F, Sonka M, Buatti J, Aylward S, Miller JV, Pieper S & Kikinis R. 2012. 3D Slicer as an image computing platform for the Quantitative Imaging Network. Magn. Reson. Imaging 30: 1323–1341.

Fisher JB & Tomlinson PB. 2002. Tension wood fibres are related to gravitropic movement of red mangrove (*Rhizophora mangle*) seedlings. J. Plant Res. 115: 39–45.
Foster AS. 1956. Plant idioblasts: Remarkable examples of cell specialization. Protoplasma 46: 184–193.
Fromm JH, Sautter I, Matthies D, Kremer J, Schumacher P & Ganter C. 2001. Xylem water content and wood density in spruce and oak trees detected by high-resolution Computed Tomography. Plant Physiol. 127: 416–425.
Gärtner H, Lucchinetti S & Schweingruber FH. 2014. New perspectives for wood anatomical analysis in dendrosciences: the GSL1-microtome. Dendrochronologia 32: 47–51.
Gärtner H & Schweingruber FH. 2013. Microscopic preparation techniques for plant stem analysis. Verlag Dr. Kessel, Remagen-Oberwinter.
Hervé V, Mothe F, Freyburger C, Gelhaye E & Frey-Klett P. 2014. Density mapping of decaying wood using X-ray Computed Tomography. Int. Biodeter. Biodegr. 86: 358–363.
InsideWood. 2004-onwards. Published on the Internet. http://insidewood.lib.ncsu.edu/search [accessed in October 2015].
Juncosa AM. 1982a. Developmental morphology of the embryo and seedling of *Rhizophora mangle* L. (Rhizophoraceae). Amer. J. Bot. 69: 1599–1611.
Juncosa AM. 1982b. Embryo and seedling development in Rhizophoraceae. Department of Botany, Duke University.
Kairo JG. 1995. Artificial regeneration and sustainable yield management of mangrove forests at Gazi Bay, Kenya. Department of Botany, University of Nairobi.
Krauss KW, Lovelock CE, McKee KL, López-Hoffman L, Ewe SML & Sousa WP. 2008. Environmental drivers in mangrove establishment and early development: A review. Aquat. Bot. 89: 105–127.
Lauri PE, Gorza O, Cochard H, Martinez S, Celton JM, Ripetti V, Lartaud M, Bry X, Trottier C & Costes E. 2011. Genetic determinism of anatomical and hydraulic traits within an apple progeny. Plant Cell Environ. 34: 1276–1290.
Marcelis-van Acker CAM. 1994. Ontogeny of axillary buds and shoots in roses: Leaf initiation and pith development. Scientia Horticulturae 57: 111–122.
Matthijs S, Tack J, van Speybroeck D & Koedam N. 1999. Mangrove species zonation and soil redox state, sulphide concentration and salinity in Gazi Bay (Kenya), a preliminary study. Mangroves and Salt Marshes 3: 243–249.
Metcalfe CR & Chalk L. 1957. Anatomy of the Dicotyledons: leaves, stem, and wood in relation to taxonomy with notes on economic uses. Vol. 1. Oxford University Press, Oxford, UK.
Metcalfe CR & Chalk L. 1979. Anatomy of the Dicotyledons. Ed. 2,Vol. 1. Systematic anatomy of leaf and stem, with a brief history of the subject. Clarendon Press, Oxford, UK.
Metzner R, Eggert A, van Dusschoten D, Pflugfelder D, Gerth S, Schurr U, Uhlmann N & Jahnke S. 2015. Direct comparison of MRI and X-ray CT technologies for 3D imaging of root systems in soil: potential and challenges for root trait quantification. Plant Methods 11: 1–11.
Obura DO. 2001. Kenya. Mar. Pollut. Bull. 42: 1264–1278.
Rabinowitz D. 1978. Dispersal properties mangrove propagules. Biotropica 10: 45–57.
Raven PH, Evert RF & Eichhorn SE. 2005. Biology of plants. W.H. Freeman and Company Publishers, USA.
Shi S, Zhong Y, Huang Y, Du Y, Qiu X & Chang H. 2002. Phylogenetic relationships of the Rhizophoraceae in China based on sequences of the chloroplast gene *matK* and the internal transcribed spacer regions of nuclear ribosomal DNA and combined data set. Biochem. Syst. Ecol. 30: 309–319.

Smith SM & Snedaker SC. 2000. Hypocotyl function in seedling development of the Red Mangrove, *Rhizophora mangle* L. Biotropica 32: 677–658.
Sousa WP, Kennedy PG, Mitchell BJ & Ordóñez M. 2007. Supply-side ecology in mangroves: do propagule dispersal and seedling establishment explain forest structure? Ecol. Monogr. 77: 53–76.
Spalding M, Kainuma M & Collins L. 2010. World Atlas of mangroves. Earthscan Ltd, London, Washington.
Stamm AJ & Hansen LA. 1937. The bonding force of cellulosic materials for water (from specific volume and thermal data). J. Physical Chem. 41: 1007–1016.
Subramanian S, Han L, Dutilleul P & Smith DL. 2015. Computed tomography scanning can monitor the effects of soil medium on root system development: an example of salt stress in corn. Front. Plant Sci. 6: 1–12.
Tomlinson PB & Cox P. 2000. Systematic and functional anatomy of seedlings in mangrove Rhizophoraceae: vivipary explained? Bot. J. Linn. Soc. 134: 215–231.
Tomlinson PB. 1994. The botany of mangroves. Cambridge Univ. Press, Cambridge, New York, Melbourne.
Van den Bulcke J, Boone M, Van Acker J, Stevens M & Van Hoorebeke L. 2009. X-ray tomography as a tool for detailed anatomical analysis. Ann. For. Sci. 66: 1–12.
Wilkinson HP. 1981. The anatomy of the hypocotyls of *Ceriops* Arnott (Rhizophoraceae), recent and fossil. Bot. J. Linn. Soc. 82: 139–164.
Wise RR & Juncosa AM. 1989. Ultrastructure of the transfer tissues during viviparous seedling development in *Rhizophora mangle* (Rhizophoraceae). Amer. J. Bot. 76: 1286–1298.
Witomski P, Krajewski A & Narojek T. 2010. Measurements of wood density using X-ray computed tomography. Ann. WULZ-SGGW, For. and Wood Technol. 75: 485–489.
Ye ZH. 2002. Vascular tissue differentiation and pattern formation in plants. Annu. Rev. Plant Biol. 53: 183–202.
Youssef T & Saenger P. 1996. Anatomical adaptive strategies to flooding and rhizosphere oxidation in mangrove seedlings. Aust. J. Bot. 44: 297–313.

Accepted: 18 December 2015